TECTONIC CLASSIFICATION AND GEOCHEMICAL SIGNIFICANCE OF STYLOLITES IN THE KOMETAN FORMATION (TURONIAN) IN DOKAN AREA, SULAIMANIYAH, NE IRAQ

Khaldoun S. Al-Bassam[1] and Saffa F.A. Fouad [2]

Received: 4/ 12/ 2011, Accepted: 5/ 4/ 2012
Key words: Stylolites, Kometan Formation, Iraq

ABSTRACT

Stylolites of the Kometan Formation are genetically studied and classified in this paper. Mineralogy and chemistry of the stylolite-seam residual deposits were investigated. Mass and thickness reduction of the limestone, due to pressure-solution, were estimated by geometric and chemical criteria methods.

Sedimentary stylolites and younger tectonic stylolites were identified, in addition to several mesoscopic, younger reverse and normal faults, and different types and sets of veins with various age relationships relative to the stylolites. Residual deposits of the stylolite seams are composed of quartz, orthoclase, illite and glauconite. Diagenetic cementation by calcite, pyrite and bitumen is abundant, whereas chert and pyrite nodules are common along the stylolite seams. The least mobilized elements during stylolitization are Ti, Al and K, followed by Fe, Si, Cr and U, whereas Ca, Na, Mg, Mn and Ni are mostly mobilized.

Limestone mass reduction due to pressure solution was estimated in the studied section using chemical criteria, by about 5%, whereas limestone thickness shortening was estimated by about 15 cm / one cm stylolite seam thickness using two independent means: (1) geometric methods and (2) chemical and bulk density parameters. The difference in the estimated values is negligible despite the significant variation in the seam thickness and bulk density of the residual deposits as well as the uncertainty of the exact age relationship between the stylolite seams and the segmented cross-cutting veins.

تصنيف ودلالة الستايلولايت الجيوكيميائية في تكوين كوميتان (التوروني) في منطقة دوكان، السليمانية، شمال شرق العراق

خلدون صبحي البصام و صفاء الدين فخري فؤاد

المستخلص

تمت دراسة وتصنيف تراكيب الستايلولايت في تكوين كوميتان في منطقة دوكان شمال شرق العراق، إضافةً الى دراسة كيميائية ومعدنية الترسبات المتبقية على دروز الستايلولايت لغرض التعرف على نواتج إذابة الصخور الكاربونيتية المصدرية. قدرت كتلة وسمك الصخور الكاربونيتية المفقودة نتيجة لعملية الإذابة الضغطية، بوسيلتين مختلفتين هما العلاقات الهندسية والظواهر الكيميائية.

[1] Chief Researcher, GEOSURV-IRAQ
e-mail: khaldoon47@hotmail.com
[2] Expert (Structural Geology), GEOSURV-IRAQ
e-mail: saffa.fouad1957@yahoo.com

تم تحديد نوعين أساسيين من الستايلولايت وهما الرسوبي والتكتوني. الستايلولايت الرسوبي وهو الأقدم والأكثر شيوعاً في منطقة الدراسة، قسم الى نوعين: ستايلولايت سطوح التطبق والستايلولايت الداخلي الموازي لسطوح التطبق بينما قسم الستايلولايت التكتوني الى الستايلولايت الاعتيادي والسليكولايت نادر التواجد. وقد تم تحديد الأعمار النسبية للستايلولايت والتراكيب الثانوية كالصدوع والفواصل والعروق المرافقة لها وتبين أن الستايلولايت الرسوبي هو الأقدم عمراً نسبةً للتراكيب المرافقة الأخرى. كما تم تحديد أنواع مختلفة من العروق لها أعمار مختلفة بالمقارنة مع الستايلولايت، وقد تبين أن العروق العمودية ذات الملئ المعدني الليفي المتزامن هي الأكثر شيوعاً وهي متزامنة مع الستايلولايت من حيث النشأة.

تبين أن الترسبات المتجمعة على دروز الستايلولايت تتكون من معادن الكوارتز والاورثوكليز والألايت والغلوغونايت. كما حدثت عملية السمنتة بواسطة الكالسيات والبايرايت والبتيومن على البعض من هذه الدروز، إضافةً الى هذا تشكلت وتجمعت عقد من الصوان والبايرايت بامتداد الدروز. أكثر العناصر المتبقية على رواسب الدروز هي Ti، Al، K ويتلوها Fe، Si، Cr، U بينما اعتبرت العناصر Ca، Mg، Mn والى حد ما Ni الأكثر ذوباناً وحركية.

تم تقدير الكتلة الذائبة على دروز الستايلولايت في مقطع الدراسة بالطريقة الكيميائية بمقدار 5% وتم تقدير السمك المذاب من حجر الكلس بالطرق الهندسية والذي يتناسب بشكل عام مع سمك دروز الستايلولايت المتكونة، وتبين أنه يتطلب إذابة حوالي 15 سم من سمك الصخور الكاربونيتية لإنتاج درز بسمك 1 سم. أظهرت الطرق الكيميائية المعتمدة على الكثافة الكلية والفقدان بالكتلة تقديرات مشابهة للطرق الهندسية مما يعطي هذه التقديرات موثوقية عالية على الرغم من اختلاف سمك الدروز من مكان الى آخر وكذلك اختلاف الكثافة الكلية للرواسب المتجمعة على الدرز فضلاً عن مدى دقة تحديد علاقة الأعمار النسبية بين العروق القاطعة والستايلولايت.

INTRODUCTION

▪ Kometan Formation

The Turonian Kometan Formation consists of light grey, thinly bedded, tough limestone. Some silicified and glauconitic beds are also present particularly in the lower part. The formation, which is thought to have deposited in different environments ranging from shallow shelf to open marine, exhibits variable thickens, but generally does not exceed 300 m. (Jassim and Goff, 2006).

The formation is widely exposed in northeastern Iraq and around Sulaimaniyah City in particular. In a fresh road cut in Dokan area some 60 Km to the northwest of Sulaimaniyah City, the middle part of the formation is well exposed around the northwestern plunge of Sordash anticline, close to Dokan Dam Lake (Fig.1). The beds exhibit an extensive stylolitization through the entire exposed rock column. The studied part of the exposed section is about 25 m thick and the samples were collected from about 4 m thick sequence.

▪ Stylolites

Carbonate rocks may undergo substantial low-temperature deformation by dissolution along bedding planes and preexisting fractures that are subject to compression. The process is known as pressure-solution (Suppe, 1985 and Ramsey and Huber, 1983).

Pressure-solution is a deformation process by which soluble rock material under stress goes into solution at localized points where the stress is maximum. The dissolved material, which is transported by flow or diffusion (Ramsey and Huber, 1983 and Roland *et al*., 2007), may precipitate in nearby low-stress sites (such as veins and pores) in the rock system or transported completely out of the system. Accordingly, the geometric effects of pressure-solution can be complex, and may or may not lead to significant volumetric changes (Ramsey and Huber, 1987).

As a result of rock dissolution, distinct seams of dark color arise from the accumulation of the relatively insoluble components in the rock (such as clays, organic matter, iron oxides,

etc.) on the surfaces were dissolution took place. These surfaces of dissolution, however, are highly irregular due to asymmetric dissolution of the rock and show a characteristic saw-tooth profile and interlocking cone-like form in three dimensions. The long axes of these teeth and cones are usually perpendicular to the surface of dissolution (exceptions do occur). The shape, size amplitude and extension of the stylolite are extremely variable, and depending on many factors including rock type, homogeneity, impurities, grain size, temperature, strain rate, gravitational load and tectonic stresses (Park and Schot, 1968; Dunne and Hancock, 1994 and Van der Pluijm and Marshak, 1997).

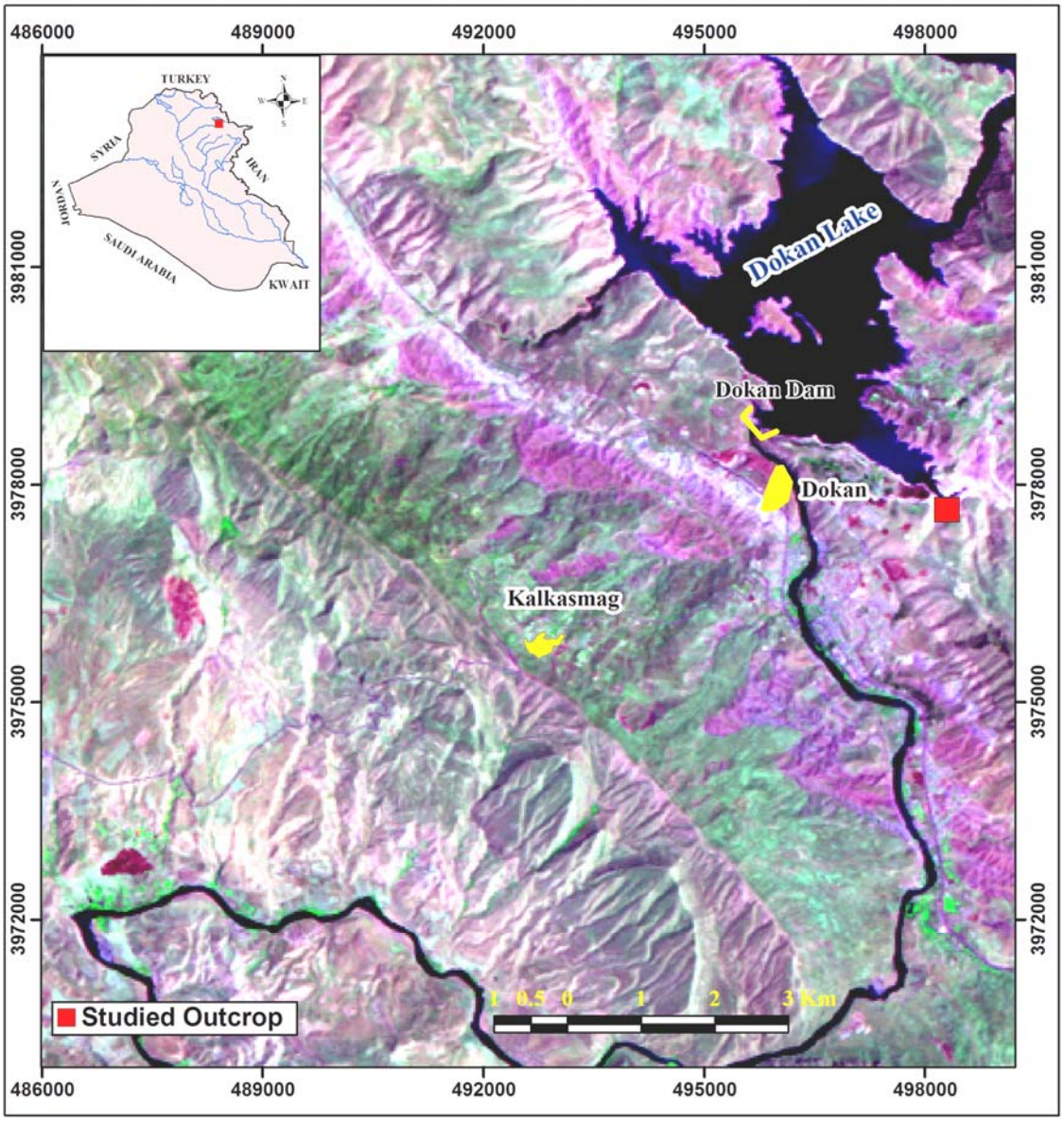

Fig.1: Location of the study area (Landsat TM image, 2010 RGB 742)

- **Stylolites as paleostress indicator**

Stylolites and the associated veins are considered as a significant mesoscopic paleostress indicators (Dunne and Hankock, 1994). In a certain stress condition, such as that shown in Figure (2), stylolite surface normally occur perpendicular to the maximum principal compression (σ 1) whereas the stylolite columns (or the long axes of the teeth and cones) are usually form parallel to it. The associated extensional veins usually form parallel to the maximum principal compression (σ 1) and perpendicular to the least principal compression (σ 3). Therefore, stylolites define the places of maximum shortening and volumetric loss, and the associated veins define the places of maximum elongation and volumetric increase (Suppe, 1985; Ramsey and Huber, 1983 and 1987 and Dunne and Hancock, 1994).

Many rocks, however, may undergo considerable deformation by dissolution along bedding planes and preexisting fractures that are subject to more than one cycle of compression. Accordingly in the structural and paleostress analysis it is more practical to classify the stylolites according to their mode of origin rather than their geometric shape and appearance.

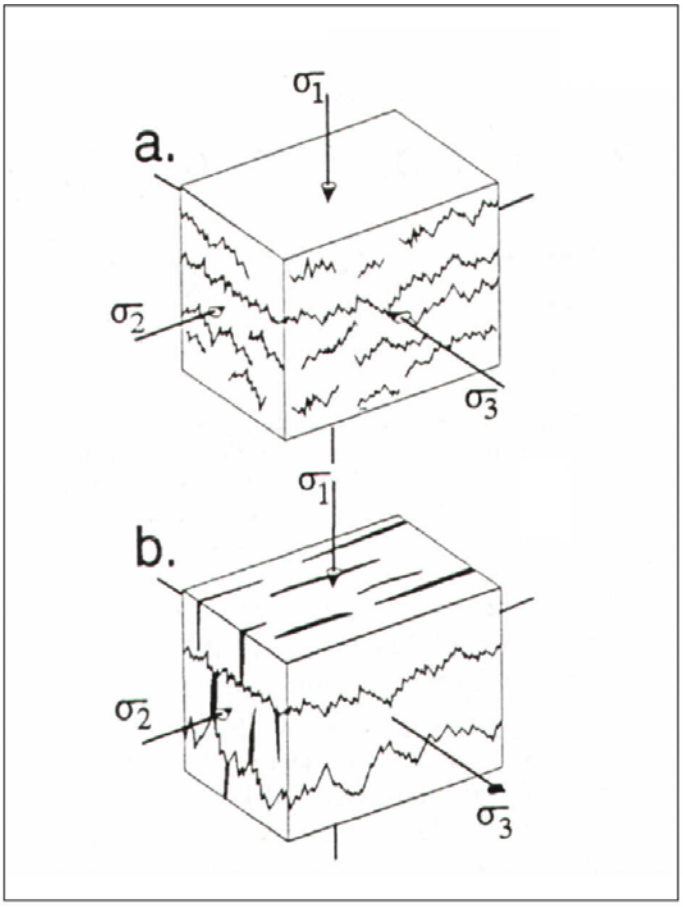

Fig.2: **a)** Principal stress axes inferred from stylolite seams with surface-normal columns,
b) Principal stress axes inferred from coeval orthogonal stylolite seams
and extensional veins.
σ 1, σ 2, σ 3 : are maximum, intermediate, and minimum compressive stresses respectively
(after Dunne and Hancock, 1994)

PREVIOUS WORK ON STYLOLITES IN IRAQ

Surface exposures in the Iraqi part of Zagros Fold Thrust Belt are dominated by carbonates and sandstones outcrops. The rocks were folded and faulted to different degrees, and contain considerable mesoscopic (outcrop scale) deformational features. These features are faults, joints, veins, stylolites, etc. Though well developed in carbonate and sandstone rock types, mesoscopic stylolites were the least to receive the attention of Iraqi researchers.

- Perhaps the first serious study was conducted by Fouad (1983) who have considered pressure-solution as important deformational mechanism in Qara Chuq folds development, after calculating the relative volumetric losses that occurred on the associated stylolites.

- Balaky (2006) mentioned the presence of sutured-seam and non-sutured seam stylolites in the Harur Formation at Nazdur Village, NE Zakho. He attributed the stylolites to chemical compaction (pressure solution) digenetic processes.

- Sherwani and Balaky (2006) described sutured seam stylolites within the cherts of Sargelu Formation and used their presence as evidence of a diagenetic origin of the black chert beds found in the upper part of the formation.

- In his study of chert nodules in Kometan Formation in Dokan area, Al-Barzinjy (2008) tried to explain the stylolitization in the area, with emphasis on bedding-type stylolites.

- Recently Daoud *et al*. (2010) described stylolitization in the Balambo Formation at Azmer Mountain (Sulaimaniyah) and identified two types: sutured with small amplitude and sutured with high amplitude, both formed in limestone of low insoluble residue content, under overburden pressure.

WORK PROCEDURES

- **Sampling and field observations**

Two field trips were made to the area for outcrop study and sampling. Twenty five samples were collected from a road-cut section in the Kometan Formation within Dokan Lake vicinity where well developed, simple wave-like, parallel to bedding and smaller scale, sutured stylolites are exposed (Fig.3). Minor oblique and vertical veins are abundant, cutting through the stylolite seams. Some appear to have formed earlier or during the stylolite development and others have formed later Orthogonal veins with calcite cement are common.

The sampling included the limestone of the Kometan Formation and the stylolite seam deposits, as well as the calcite veins cement. The limestone is white, very tough, medium to thinly bedded, with chert nodules, several centimeters in size, especially abundant, as horizons along the stylolite seams (Fig.4). The stylolite seams are few millimeters to about 3.5 cm thick. The filling residual materials are flakey, reddish brown, friable, ferruginous, with pyrite, bitumen and calcite cements (Fig.5). Pyrite nodules were noticed in close contact with the stylolite seams (Fig.6).

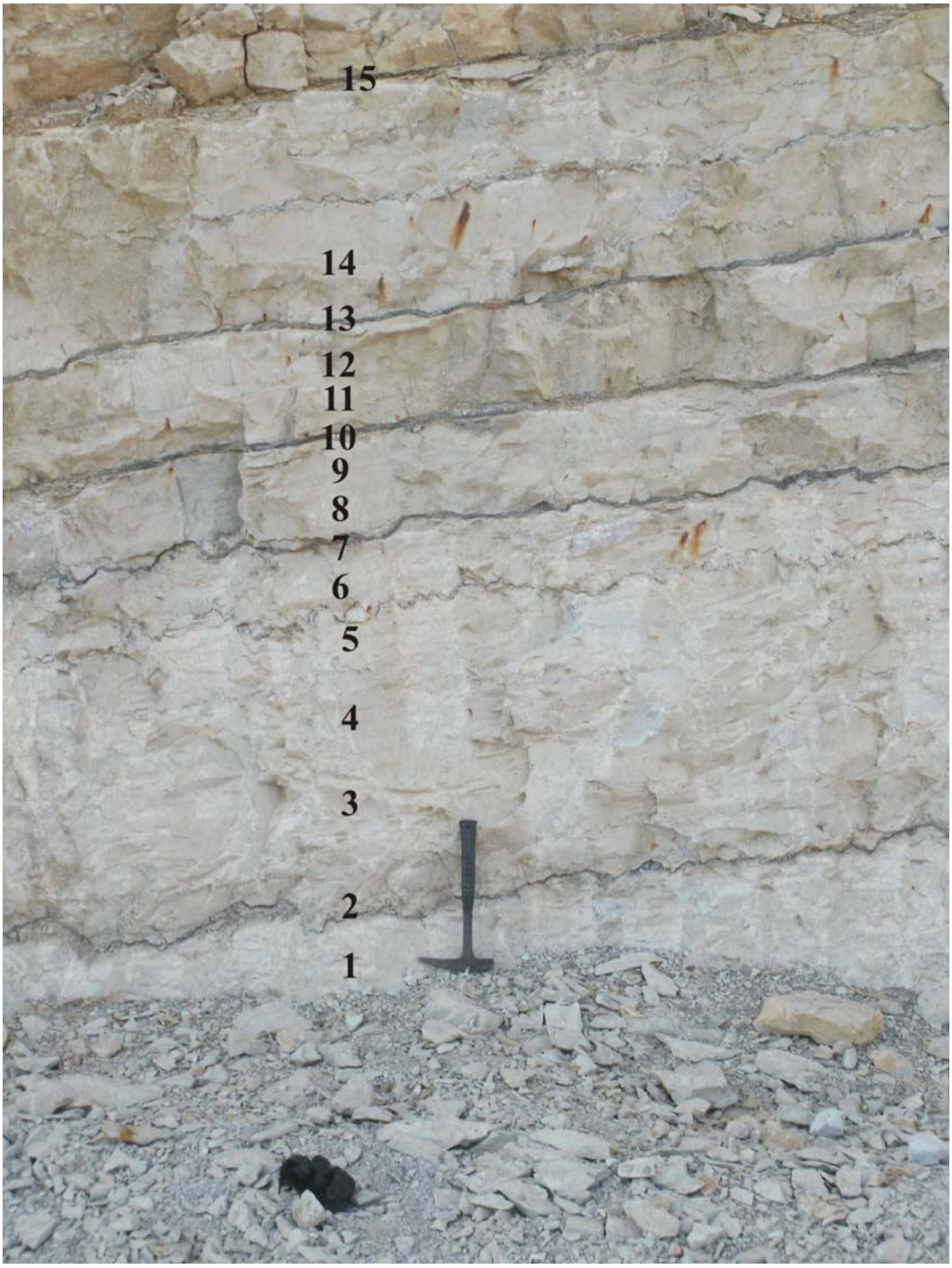

Fig.3: Studied section and samples location
(numbers location indicate sampling points)

Fig.4a: Isolated chert nodules along stylolite seams

Fig.4b: Adhered chert nodules along stylolite seams

Fig.5: Details of stylolite seam deposits

Fig.6: Pyrite nodules along stylolite seams

▪ **Laboratory work**

Twenty thin sections were prepared and studied by optical microscopy (occasionally more than one thin section was prepared from the same sample). Most of them are from the limestone beds. The stylolite residual deposits were difficult for thin section preparation, being highly friable, but a few thin sections were prepared especially to study the nature of calcite in these samples. A few thin sections were also studied from the vein-filling calcite. Two stylolite residual sediments samples were examined by X-ray diffraction for mineral composition. Bulk samples and clay fraction were analysed (Table 1).

Ten limestone samples and five stylolite residual deposits were analysed for major and some trace elements, using standard GEOSURV work procedures (Al-Janabi *et al*., 1992). The chemical analysis included the followings (Table 2): SiO_2, Fe_2O_3, Al_2O_3, CaO, MgO, K_2O, Na_2O, L.O.I., Cr, Ni, Ti, Mn and U. One Kg sample of stylolite-free limestone of the Kometan Formation was digested with 10% HCl until the carbonate was completely removed and the insoluble residue was collected, dried and the weight accurately determined. The insoluble residue was analyzed for the same elements as above and was examined by X-ray diffraction. The bulk density of 6 samples was determined using GEOSURV Work Procedure, Part 19 (Al-Haimus, 1994). They included 4 samples from various stylolite seams residue and 2 samples from the parent limestone neighboring the sampled stylolite seams (Table 3).

RESULTS OF LABORATORY INVESTIGATIONS

– Petrography: The limestone samples studied show a planktonic forminiferal wackestone to packstone, rich in Hetrohelicidae (Fig.7). It represents a typical deep marine (basinal) facies. Pyrite digenetic replacement of the micrite is common, not affecting the fossil shells (Fig.8). The vein filling is composed of spary calcite cement (Fig.9). The calcite cement was also noticed within the stylolite seams deposits in considerable amounts and it represents the only form of carbonate in the studied stylolite seams deposits. No remains of the parent limestone were noticed in the examined samples. (Fig.10). Bitumen is occasionally present, as impregnation with the calcite cement, in some stylolite residual deposits (Fig.11). Microstylolites (< 0.1 mm thick) are occasionally encountered in the limestone samples (Fig.12). Evidence of deformation due to strain and stress are common in the limestone as well as in the calcite cement.

– Mineralogy: Calcite dominates the mineral composition of the Kometan Formation in the sampled section, with minor amounts of quartz (chalcedony) and pyrite. The weak-acid insoluble residue of the limestone shows similar mineral composition to that of the stylolite residual deposits including quartz, K-feldspar, hematite, illite, glauconite and kaolinite (Table 1 and Fig.13). Calcite and traces of gypsum are only found in the stylolite deposits (Fig.14). The X-ray diffractograms of the clay fraction of the stylolite deposits and the limestone insoluble residue show, beside illite and glauconite basal (001) reflections, some mixed layer minerals (Fig.13b), which may be due to interstratified glauconite-smectite and/ or illite-smectite. (Thompson and Hower, 1975).

Table 1: Mineral analysis by X-ray diffraction

Sample No.	Non – clay minerals	Clay minerals
7	Calcite, quartz, orthoclase, hematite, gypsum (trace)	Illite, glauconite, kaolinite
10	Calcite, quartz, orthoclase, hematite	Illite, glauconite, kaolinite
I.R.	Quartz, orthoclase, hematite	Illite, glauconite

– Chemical composition: The analytical results are shown in Table (2). The limestones, with about 52% CaO, indicate more than 92% $CaCO_3$. The results of the ten limestone samples analysed is monotonous and show little variation. The weak-acid insoluble residue of the limestone is 4.75 weight % of the total limestone constituents. It is composed mainly of silica, followed by Al_2O_3 and K_2O which corresponds well with the mineralogy of the insoluble fraction. The concentrations of Al_2O_3, Fe_2O_3, K_2O and TiO_2 in the acid-insoluble residue were enriched by about 15 times relative to their concentrations in the limestone host rock, whereas silica enrichment approaches about 20%. The sum of SiO_2, Fe_2O_3, Al_2O_3, TiO_2, and K_2O in the limestone samples is about 5% (mean value), which is comparable to the IR content determined by weak-acid dissolution of the limestone of 4.75%.

Table 2: Chemical analysis of the limestone and stylolite seam deposits samples

Sample No.	SiO_2	TiO_2	Fe_2O_3	Al_2O_3	CaO	MgO	K_2O	Na_2O	SO_3	L.O.I	Mn	Ni	Cr	U
	(%)										(ppm)			
1	3.44	0.03	0.17	0.94	52.22	0.77	0.29	0.01	n.a.	41.68	48	14	8	0.55
3	3.69	0.03	0.13	0.88	51.97	0.90	0.26	0.02	n.a.	41.70	53	15	10	0.50
4	3.48	0.03	0.13	0.59	52.35	0.96	0.18	0.02	n.a.	41.90	52	12	7	0.30
5	4.44	0.04	0.14	0.87	51.74	0.75	0.26	0.02	n.a.	41.35	61	13	8	0.40
6	2.85	0.03	0.12	0.57	52.80	0.81	0.18	0.02	n.a.	42.23	72	12	7	0.55
8	4.28	0.04	0.26	1.15	51.12	0.82	0.37	0.02	n.a.	41.48	52	15	10	0.30
9	3.26	0.03	0.75	0.94	51.37	0.81	0.29	0.03	n.a.	41.67	62	15	9	0.40
11	3.05	0.03	0.21	0.84	51.41	0.84	0.28	0.02	n.a.	41.91	61	17	9	0.32
12	4.11	0.03	0.25	1.14	51.42	0.86	0.42	0.03	n.a.	41.20	71	16	8	0.60
14	3.10	0.03	0.20	0.81	52.26	0.85	0.28	0.02	n.a.	41.97	73	14	7	0.50
2	10.06	0.08	22.01	2.25	28.57	0.35	0.72	< 0.02	26.24	9.50	29	39	9	0.15
7	37.89	0.56	2.57	13.25	17.39	1.52	4.89	0.07	n.a.	19.37	56	56	64	4.75
10	32.40	0.46	2.39	10.99	23.28	1.49	4.05	0.05	n.a.	23.10	63	54	86	1.85
13	35.70	0.56	2.85	12.79	19.01	1.53	4.63	0.06	n.a.	20.41	68	55	91	3.45
15	16.48	0.29	1.63	6.92	37.49	1.28	2.26	0.03	n.a.	32.83	69	38	55	1.80
I.R	70.63	0.43	3.48	11.63	1.53	1.08	4.52	0.17	1.21	4.53	25	31	55	0.8

n.a. = not analysed
Samples: 1, 3, 4, 5, 6, 8, 9, 11, 12 and 14 are limestones.
Samples: 2, 7, 10, 13 and 15 are stylolite seam deposits.
I.R. Insoluble residue remained after weak – acid digestion of the limestone.

Table 3: Bulk density determination (gm/cm^3)

Sample	Description	Bulk density
a	Stylolite seam deposits with calcite cement	2.444
b	Stylolite seam deposits with calcite cement (minor seam within limestone bed no.14; see Fig.3).	2.412
c	Stylolite seam deposits with bitumen (stylolite seam no.2; see Fig.3).	1.323
d	Stylolite seam deposits with calcite cement (seam no.15, see Fig.3).	2.193
e	Limestone, Kometan Formation	2.536
f	Limestone, Kometan Formation	2.533

The chemical analysis of the stylolite seams deposits show more variation. Samples 2 and 15 are not in harmony with the other three samples, which have close chemical composition. In these three samples, the CaO content indicates the presence of about 35 wt% calcite (secondary), and about 50 wt% of illite, glauconite and other mixed-layer clay minerals, in addition to about 5% quartz.

The analysis of sample 2 shows higher content of Fe (as Fe_2O_3) and S (as SO_3), most probably related to pyrite anomalous presence in this sample, approaching about 20%, as well as its oxidation products of Fe oxyhydroxides. This sample also contains high amount of calcite, approaching about 50% of the mineral constituents. About 10% illite and glauconite and (5 – 10) % quartz may be inferred from the analysis. Sample 15 contains the highest calcite content among the stylolite deposits samples, approaching about 70%, accompanied by about 30% of illite and galuconite (based on chemical analysis).

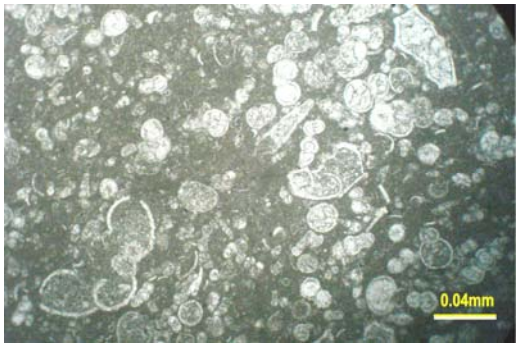

Fig.7: Texture of the limestone (sample 3) (ppl)

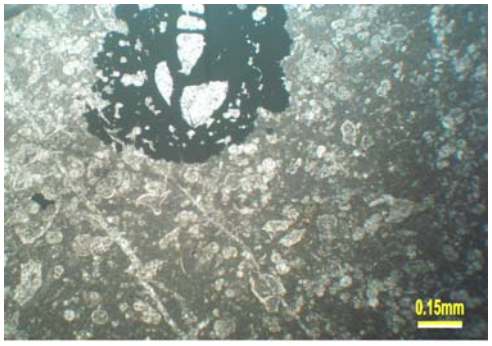

Fig.8a: Pyrite replacement of micrite (sample 14) (ppl)

Fig.8b: Pyrite replacement of micrite (sample 14) (binocular)

Fig.9: Calcite syntaxial vein fill (ppl) (see Fig.18)

Fig.10: Calcite cement in stylolite seam (sample 15) (ppl)

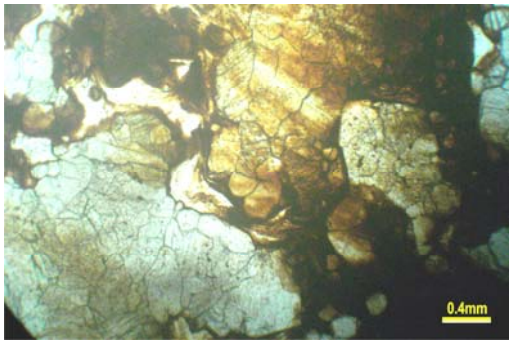

Fig.11a: Bitumen impregnation of calcite cement in stylolite seam (sample 2) (ppl)

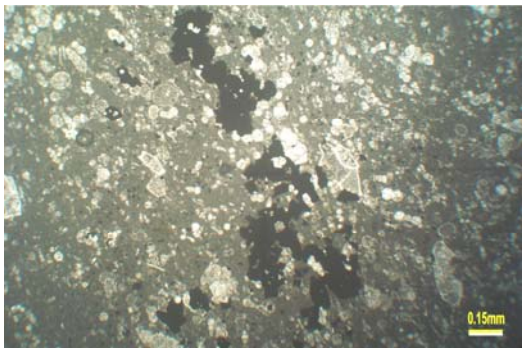

Fig.11b: Bitumen impregnation of the limestone (sample 8) (ppl)

Fig.12: Microstylolite in the limestone (sample 9) (ppl)

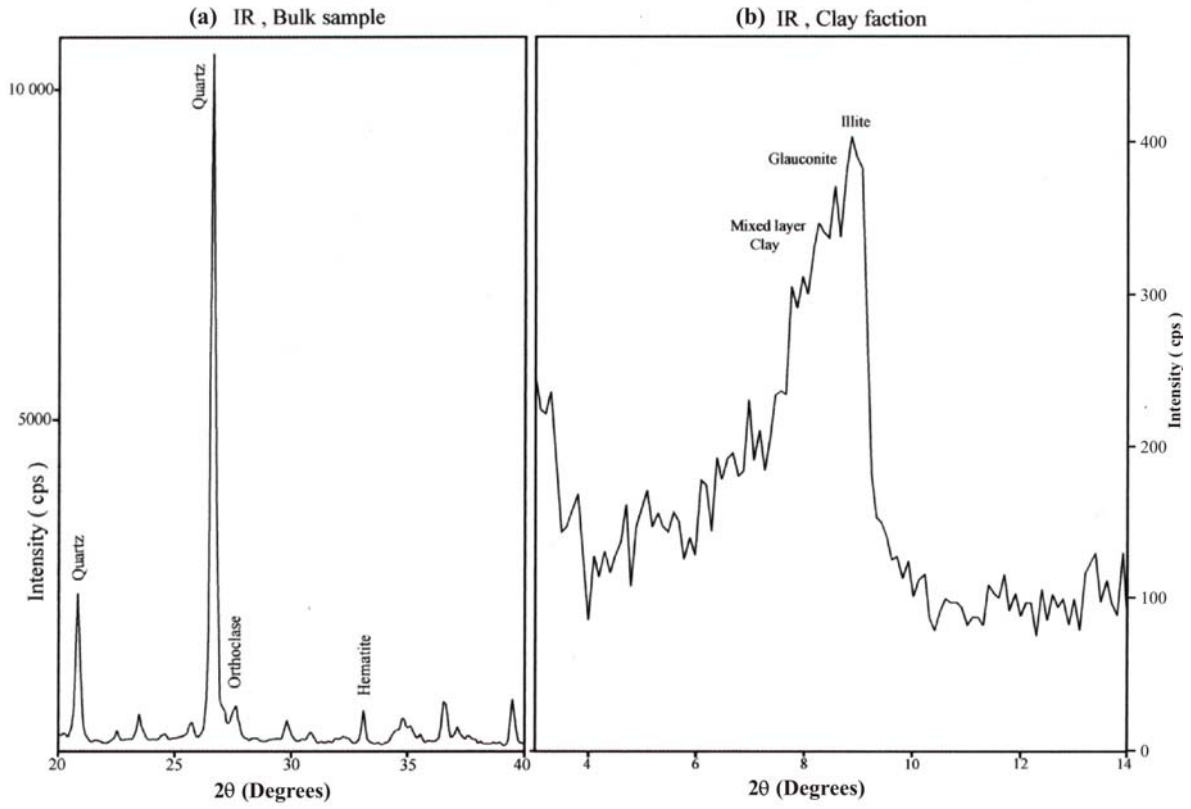

Fig.13: X-ray diffractograms of weak-acid insoluble residue (IR)

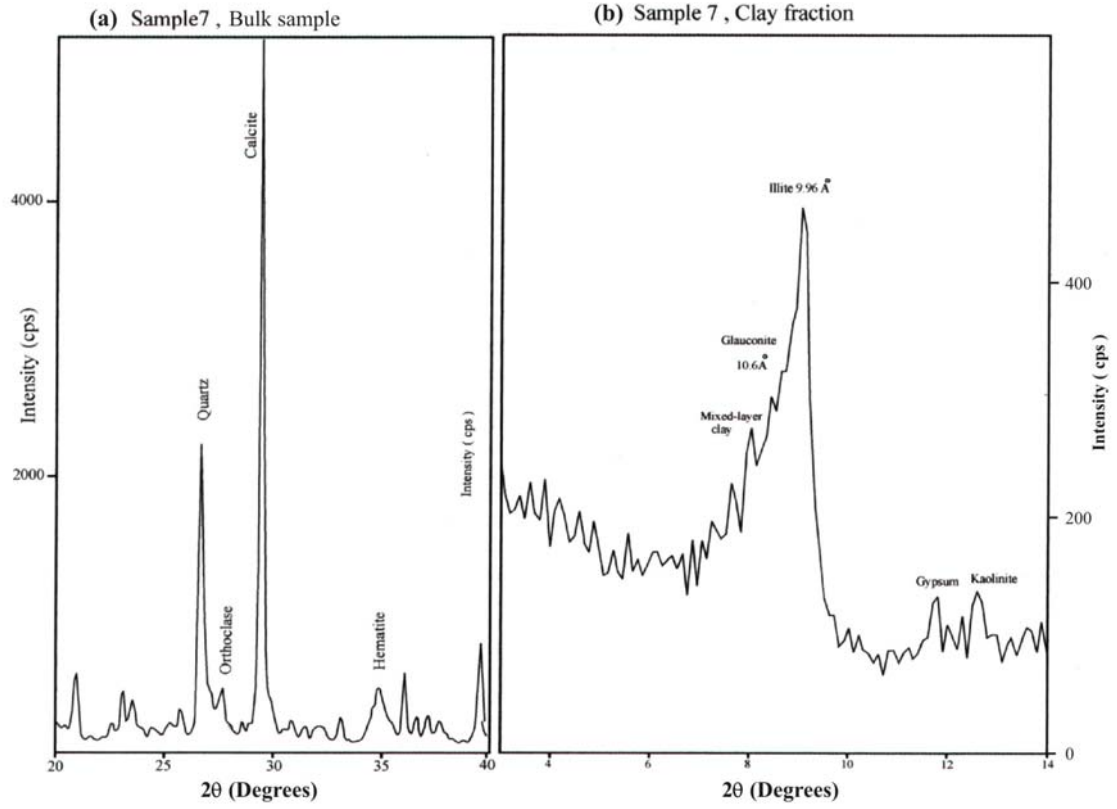

Fig.14: X-ray diffractograms of stylolite seam deposits

Fig.15: Bedding stylolite (lower) and bedding-parallel stylolite (upper)

Fig.16: Vertical tectonic stylolite terminated on a bedding stylolite

Fig.17: Younger normal faults cross-cut the bedding stylolite seams

Fig.18: Orthogonal syntaxial vein with fibrous calcite fill

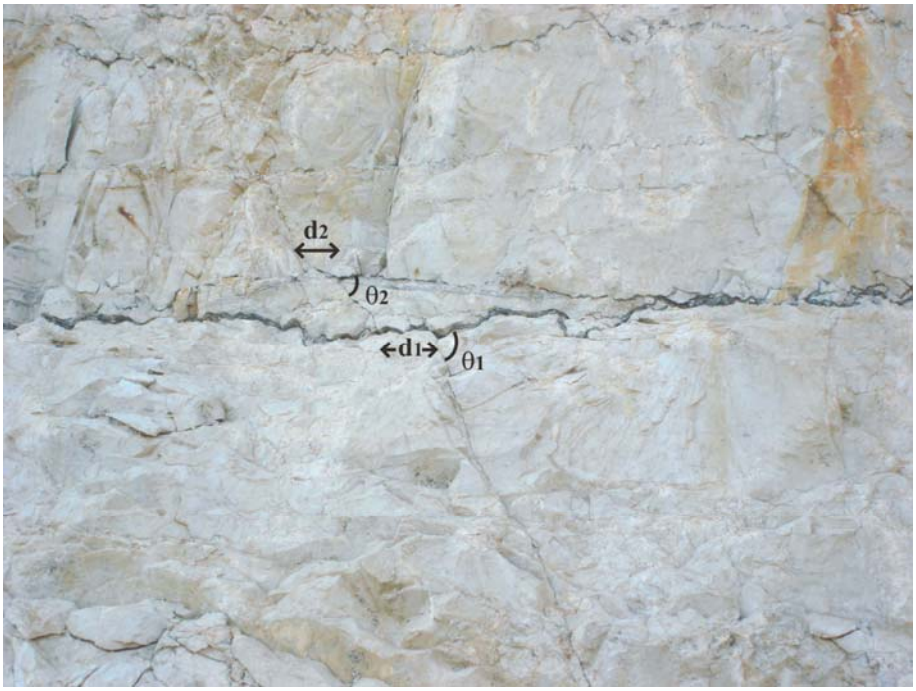

Fig.19: Previously continuous vein, segmented by pressure-solution surfaces

d: apparent slip (d1 = 18cm, d2 = 10cm),
Θ: angle of intersection between the vein and the stylolite seam (Θ1 = 60º, Θ2 = 55°)
$Ws_1 = d_1 \tan \Theta_1 = 18x1.7 = 30.6$ cm
$Ws_2 = d_2 \tan \Theta_2 = 10x1.4 = 14.0$ cm
Ws = Width (thickness) of the dissolved limestone strip

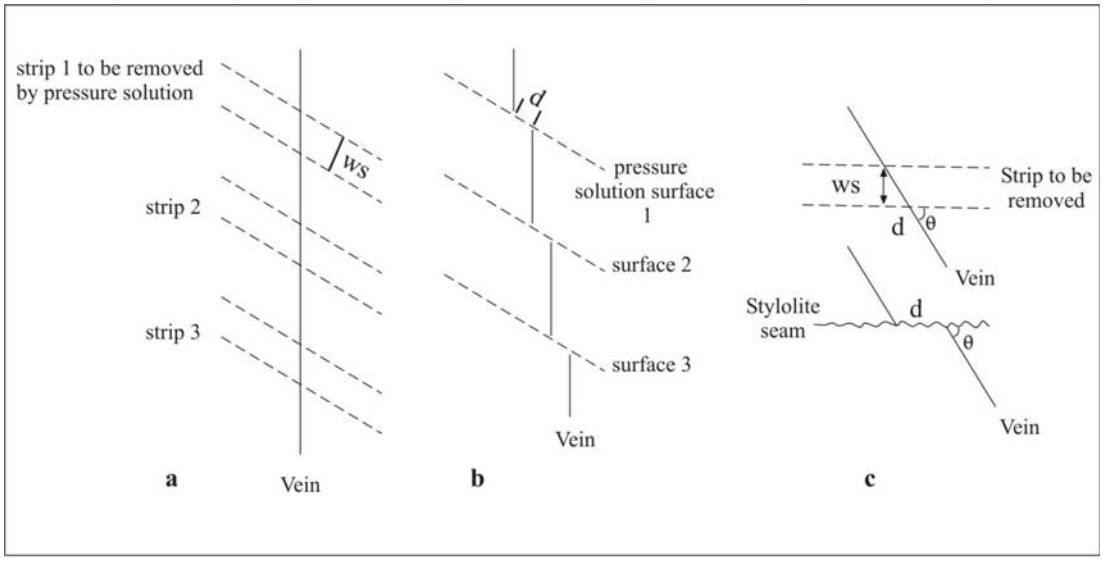

Fig.20: Geometric arrangement of segmented vein by pressure – solution surface
a) before solution, **b)** after solution, **c)** enlargement of (b) showing:
(d) apparent slip, (θ) angle of intersection, (ws) width of the dissolved strip

DISCUSSION

▪ Stylolites classification

Stylolites that have developed in Kometan Formation in the study area were classified according to their origin into two types; sedimentary stylolites and tectonic stylolites.

▪ Sedimentary stylolites

These are the most commonly observed stylolite type in the study area composing about 85% of the total recorded seams. Sedimentary (or diagenetic) stylolites are usually parallel or sub-parallel to the bedding planes of the sediments and it is believed that they formed as a result of gravitational loading during diagenetic compaction (Ramsey and Huber, 1983). This is well inferred from the geometry of the stylolite columns (teeth and cones) which are perpendicular to the bedding and parallel to the direction of gravitational loading at the time of their formation (i.e. vertical when bedding are restored to the horizontal position). Sedimentary stylolites are well developed in Kometan Formation. They occur either along the bedding planes of the rock units, (will be referred to hereafter as "bedding stylolites") or parallel to the bedding but within the body of the rock horizon (will be referred to hereafter as "bedding parallel stylolites"). Though they formed under identical geological condition, they reflect a substantially different appearance, and consequently will be described hereinafter separately in purpose of showing more details.

– Bedding stylolites: They are the commonest and the most extensive stylolite type in the formation. They were developed along the entire exposed planes of the successive rock units of the Kometan Formation (Fig.15). They extend continuously for long distances (more than 100 m) along the whole exposed beddings without any primary interruptions. Nevertheless, they were cross-cut by some late formed mesoscopic faults and fractures. The stylolite seams are abnormally thick and vary between 0.5 cm and 3.5 cm. They are composed of dark brownish grey insoluble residue; consist of clays, calcite cement, bituminous material, iron oxide and pyrite. The stylolite seams are often bordered by chert nodules with different sizes and shapes.

The amplitudes of the columns vary between 1 cm up to 10 cm. The geometric shape of the column vary between peaked, when the seams are thin, through hummocky to wavy when the seams are thick. Similar observations were reported by Van der Pluijm and Marshak (1997) where they attributed it to the amount of clay content.

– Bedding parallel stylolites: They are similar to the bedding stylolites, except that they were formed within the body of the sedimentary units and not along their bedding planes (Fig.15). They are parallel to subparallel to the bedding, extending for few meters, then either bifurcate, die out, or truncated by other structures. The stylolite seams are dark brownish gray to black in color and are usually thin and rarely exceeds 0.25 cm in thickness. Chert nodules are also found associated with the seams but usually smaller in size and lesser in number than those associated with the bedding stylolites. The amplitude of the seams is usually less than 2 cm, whereas their shape vary between sutured to sharp-peaked.

▪ Tectonic stylolites

This type of stylolites is formed in response to tectonic compression rather than gravitational loading. They usually initiate perpendicular to the maximum compressive tectonic stress. As a result, they might be at any angle to the bedding planes, and might intersect and displace primary or early formed tectonic features of the rock (Ramsey and Huber, 1983). Tectonic stylolites in the study area can be subdivided into; normal (or vertical) stylolites and slickolites (or oblique stylolites).

– Normal stylolites: These stylolite surfaces occur at right angle to the bedding planes, with interlocking teeth and cones (columns) having their long axes oriented perpendicular to the stylolite surfaces and parallel to the bedding planes of the sedimentary units (Fig.16). As inferred from their orthogonal angular relationship to the bedding and the orientation of their columns, they indicate layer-parallel shortening in response to the regional horizontal maximum compression responsible for the folding in the area.

This type of stylolites is usually restricted between the bedding surfaces of the individual bed (i.e. strata bound), and not observed to pass through more than one bed. stylolite seams are usually dark gray to black, thin (average 0.1 cm thick), sutured to sharp-peaked in shape with amplitudes rarely exceeds 1 cm. Chert nodules are formed associated with this type of stylolite but they are rare and very small in size in comparison with these associated with the previously described stylolite types.

– Slickolites: Slickolites are stylolites that are inclined to the bedding at any angle rather than perpendicular to it (Ramsey and Huber, 1983 and 1987). In the study area however, they are very rare and very few were observed. Accordingly they were excluded from the present analysis.

▪ Stylolites and their relationship to other mesoscopic structures

Kometan Formation exhibits a variety of mesoscopic structures beside the stylolites. These mesoscopic structures include faults, veins, fissures and joints. Several mesoscopic reverse and normal faults have been observed to cross-cut and displace the sedimentary stylolites (bedding stylolites and the bedding parallel stylolites) indicating their younger age relative to that of stylolites (Fig.17). Joints and fissures usually intersect the sedimentary stylolites indicating their relative younger age too. On the other hand, the tectonic stylolites are usually found enclosed between the bedding surfaces of the individual sedimentary layer and not observed to propagate across them to the next layer. In other words, the tectonic

stylolites always terminate against the bedding stylolite. This abutting relationship implies that the tectonic stylolites were formed later and are younger than the sedimentary stylolites.

Veins exhibit more complex geometric relationship with the stylolites. Different types and sets of veins with difference of relative age relationships were developed in the Kometan Formation. Nevertheless, veins perpendicular to the bedding (orthogonal veins) are the dominant type. It is observed that the sedimentary stylolites and the orthogonal veins often cross-cutting each other in Kometan Formation. Most of the orthogonal veins in Kometan Formation are of the syntaxial fibrous fill type (Fig.18). Syntaxial vein fibers grow from the walls towards the center of the vein and eventually, the fibers meet unevenly at a central seam (Durney and Ramsey, 1973). The long axes of the fibers, which are denoting the growth direction, are usually parallel to vein-opening direction (Ramsey and Huber, 1983 and Dunne and Hancock, 1994).

Orthogonal veins form as a result of vertical maximum compression and horizontal minimum compression as indicated by the layer-parallel fibers growth, which follow the extension direction. Such a causative stress system is identical to that responsible for the formation of the sedimentary stylolites (Fig.2). Similarity of the causative stress system and the mutual cross-cutting relationship, support the inference that the sedimentary stylolites and the orthogonal veins (with the syntaxial fibrous fill) were formed synchronously in the Kometan Formation.

Veins older than the sedimentary stylolites were also recorded, but they are extremely rare. Of this type is the one shown in Figure (19) were the volumetric losses were estimated. Veins formed later in the deformational history of the area are beyond the scope of the present work.

▪ **Deposits of the stylolite seams**

– Mineralogical alterations: The results obtained in this work indicate several facts that have had direct control on the development of the stylolite deposits following the dissolution of the parent limestone of the Kometan Formation by compressive burial load pressure. The main observations are that significant amounts of calcite were diagenetically reprecipitated in the stylolite seams forming essential part of the filling material. The analysis indicates that about 30 – 70% by weight of the stylolite deposits are composed of calcite cement in the studied samples. Moreover, pyrite was developed and occasionally formed a major constituent of the stylolite seam deposits (e.g. sample 2 with about 20% pyrite).

These diagenetically formed minerals have diluted the original residual materials left after the dissolution of the parent limestone and have occupied significant volume and space within the stylolite seams. The original residue consisted of orthoclase, feldspar, illite, glauconite and quartz.

The presence of these diagenetically formed minerals, as well as the bitumen impregnation of the stylolites, indicate a porous and permeable environment within the bedding planes at various stages of the stylolite development. The excess Ca^{2+} produced by pressure dissolution of the limestone have continuously penetrated the fractures, veins, and fault plains in the parent rock and formed calcite cement. Whereas, some of the mobilized silica may have been redeposited, as chert nodules, in the nearby vugs.

▪ **Dissolution and elements mobilization processes**

Dissolution of carbonate rocks under load pressure is expected to take place in an alkaline and reducing conditions. Thus, the behavior and mobility of the elements should be studied considering such environments, as well as the mineral framework hosting these elements and their stability.

The procedure described by Sastri and Sastry (1982) was used to estimate relative depletion (dissolution and mobilization) of the analysed elements in this study, as well as to estimate the mass of limestone dissolved and the mass of residue retained (Table 4).

Table 4: Chemical alterations and mass reduction calculations in wt.%
(Sastri and Sastry, 1982)

wt. (%)	Limestone	Residue	Sum=100 (%)	A	B	C	
SiO_2	3.57	35.33	36.15	2.05	1.52	42.58	F = TiO_2 limestone/ TiO_2 residue = 0.0566037
Fe_2O_3	0.24	2.60	2.66	0.15	0.09	37.50	
Al_2O_3	0.87	12.34	12.63	0.71	0.16	18.39	
TiO_2	0.03	0.53	0.54	0.03	0.0	0.0	A = F X residue analysis * = retained mass%
CaO	51.87	19.89	20.35	1.15	50.72	97.78	
MgO	0.84	1.51	1.54	0.09	0.75	89.29	
K_2O	0.28	4.52	4.63	0.26	0.02	7.14	B = Limestone analysis – A = dissolved mass%
Na_2O	0.02	0.06	0.06	0.003	0.02	100.0	
LOI	41.71	20.96	21.44	1.21	40.50	97.10	C = B/ limestone analysis X100 = percentage of dissolved mass for each oxide
	99.43	97.74	100.00	5.65	93.78		
ppm							
Mn	61	62	63.4	3.6	57.4	94.10	
Cr	8	80	81.8	4.6	3.4	42.5	* Residue analysis corrected to sum = 100%
Ni	14	55	56.3	3.2	10.8	77.14	
U	0.4	3.4	3.5	0.2	0.2	50.00	

Limestone: Mean of all limestone analysis
Residue: Mean of samples 7, 10 and 13

Comparing the analytical results of both limestone and stylolite seam deposits (Table 1), it is obvious that Ti is the least mobilized element. It seems that almost all of it has been retained in the residue. Aluminum and potassium show slightly lower competency to resist mobilization than Ti. The three elements are mainly hosted by the aluminosilicates (glauconite, illite and mixed-layer clay minerals).

Free silica, present as quartz or chalcedony, is less stable in the alkaline environment. The presence of carbonate in solution may be responsible for raising the pH to a point where quartz is more soluble and silica more mobile (Schaetzl and Anderson, 2005).

More than 40% of the original SiO_2 content of the parent limestone was mobilized during the stylolite development history, and appears that free silica have suffered the most. The silica released may be redeposited, as cementing agent. However, it is translocated only short distances, usually making films on grain surfaces, whereas carbonate cement preferentially precipitate in large voids, fractures, etc. (Schaetzl and Anderson, 2005). Some of the chert nodules, in close contact with the stylolite seams, might be of secondary origin formed by the reprecipitation of the mobilized silica.

The behavior of iron may vary, depending on its oxidation state, redox potential and the host minerals. The solubility of Fe oxides (Fe^{3+}) in alkaline environment (pH > 8) is negligible (Lindsay, 1979). However, at low Eh, Fe^{3+} may be reduced to Fe^{2+} and, therefore, becomes mobile (Korfali and Davies, 2004). In view of the digenetic formation of pyrite, it seems that considerable amounts of Fe, estimated by about 37% of the original Fe_2O_3 content present in the parent limestone, were released and mobilized. The reducing conditions needed for pyrite precipitation may have been provided by the hydrocarbon (bitumen) invasion of the stylolite porous space, (Lougheed and Mancuso, 1973).

Magnesium, Mn, Na and Ni may be incorporated in the calcite structure in substitution for Ca (Kreidler and Hummel, 1970; Veizer *et al*., 1977; Bencini and Turi, 1974 and Gad, 1969). Hence, they are bound to be released into solution while the stylolite process of formation continues. It is estimated that 77 – 100% of these elements were mobilized during the process (Table 4). On the other hand Cr and U may be shared between carbonate and aluminosilicates and for that reason they were partly mobilized (40 – 50% of their original content) (Table 4).

- **Mass and thickness reduction**

Estimation or rock mass removed by pressure solution process in certain area is rather a difficult task. Nevertheless, the width of the stylolite seam can be used as a relative measure to this estimation. Stylolite seams are the product of the accumulation of the insoluble components of the rock due to its dissolution on pressure-solution surfaces. Eventually, in a uniform lithology such as that of Kometan Formation, the more rock dissolution take place, the more insoluble residue accumulation occur, and consequently, a thicker seam will develop. Applying this simple argument on the stylolites in Kometan Formation in the study area, it become clearly evident that the bedding stylolites were the sites where relatively maximum solution and volumetric loss occurred and minimum was associated with the tectonic stylolites. This was also observed by Al-Barzinjy (2008).

Despite the fact that there is some correlation between stylolite seam thickness and the limestone reduced thickness there are some aspects that may render such correlation useless. The main factor is the porosity of the residual material and the amount of cementing material contribution to the final thickness of the stylolite, ranging, in the present case from 30% to 70% of the total mass of the stylolite deposits and stylolite thickness. Moreover, the thickness of the stylolites highly varies laterally within individual stylolite seam and also from one stylolite seam to another. Hence, such correlation may be misleading in estimating thickness reduction of the limestone.

More reliable estimate can be done on one or a number of stylolite seams, provided the presence of suitable linear geological markers. Such an estimate can only give an idea about the thickness loss in an area.

- **Estimates based on geometric methods**

As mentioned before, stylolite may cross-cut the initial rock fabric or earlier formed features. Figure (20) show an early formed vein cross-cut obliquely by number of stylolite surfaces. Due to dissolution on these surfaces, strips of rock mass will be removed, and the resultant vein segments will appear as if they were displaced laterally (Fig.20). The apparent slip (d) is a function to the angle of intersection between the vein and the stylolite surface Θ. Consequently the width (thickness) of the dissolved (or removed) rock strip (Ws) can be calculated by the equation (Hancock and Atiya, 1975): $Ws = d \tan \Theta$

Figure (19) exhibits a previously continuous vein that is now appears segmented by two stylolite surfaces. Using the above mentioned equation, the width of the removed strips can be calculated on the lower and upper stylolite surfaces respectively. It can also be noted, that the width of the seams in Figure (19) are proportional to the amount of the dissolved rock mass as mentioned earlier.

These two field examples were observed and measured in the studied outcrop. The larger displacement is 18 cm, associated with about 2 cm thick stylolite and the smaller displacement is 10 cm, associated with about 1cm thick stylolite. The geometric calculations, using Hancock and Atiya (1975) method, show that the reduction in limestone thickness by compressive load dissolution needed to produce these displacements are 30.6 cm and 14 cm respectively (Fig.19).

The geometric method to estimate thickness reduction is based on an essential assumption that the cross-cut veins or linear fractures were actuated at the same time of stylolite initiation. However, such linear fractures could have formed any time during the process of stylolite development. Fracturing is an event whereas, stylolite-seam development is a process that requires time to mature. Hence, the initiation of both phenomenon are not necessarily conjugate, and the displacement in the linear markers, used in the present estimates might show only part of the dissolution history (the later part) and the estimates of the reduced limestone thickness by this method might be lower than the actual values.

- **Estimates based on chemical characteristics**

Applying geochemical indicators to estimate mass reduction by dissolution under burial pressure is not a common or known procedure to the best of the authors knowledge. However, it has been a common practice to estimate mass changes of rocks undergone alteration or bauxitization (Sastri and Sastry, 1982). Using Ti, the least mobilized element in the studied case, to estimate mass reduction using Sastri and Sastry (1982) method is shown in Table (4). The mean chemical analysis of 10 limestone samples and 3 stylolite seam residue samples (samples 7, 10 and 13) were used in the calculations.

The results show that the remaining mass, after the dissolution of the limestone, is 5.65 wt.% and about 94 wt.% of the limestone mass was dissolved and mobilized under burial pressure. This is comparable to the insoluble residue determined by weak-acid digestion of the parent limestone which was 4.75 wt.%. It is also comparable to the sum of the relatively more resistant and less soluble oxides ($SiO_2 + Fe_2O_3 + Al_2O_3 + K_2O + TiO_2$) in the limestone which was about 5 wt.%.

In other wards each ton of limestone in the study area may have produced about 50 Kg of residual deposits remained in the stylolite seams. To convert mass reduction to thickness reduction, the bulk density of limestone and the residual deposits should be considered. The mean bulk density for the former is 2.53 gm/ cm^3 and for the latter is 2.09 gm/ cm^3 (Table 3). Converting mass reduction estimate by Sastri and Sastry (1982) method to thickness reduction of the limestone to produce 2 cm thick stylolite seam is shown in Table 5. The estimate of thickness shortening came to be about 29.2 cm.

The shortgivings of thickness estimates by this method are that the thickness (width) of the stylolite seams is highly variable laterally within individual seams and from one seam to another. Moreover, the bulk density of the measured stylolite seam deposits is also highly variable and this variation corresponds to significant differences in porosity and type of

cementing material of the seam deposits. These factors influence estimates of thickness shortening derived from chemical parameters, but not the mass reduction estimates derived by this method.

Thickness reduction estimates based on geometric method and that based on chemical characteristics show negligible differences, and they are comparable to a great extent, considering the shortgivings of both methods and the multivariables and assumptions influencing the estimate procedures in each method.

Table 5: Thickness reduction calculations derived from mass reduction estimates, based on chemical criteria

$$\frac{\text{Mass limestone}}{\text{Mass residue}} = \frac{100}{5.65} = \frac{1\text{ cm} \times 1\text{ cm} \times \text{Tlst} \times 2.53\text{ gm/ cm}^3}{1\text{ cm} \times 1\text{ cm} \times 2\text{ cm} \times 2.09\text{ gm/ cm}^3}$$

$$17.7 = \frac{2.53\ \text{Tlst}}{4.18}$$

Tlst = 29.2 cm thickness of limestone reduced to from 2 cm thick stylolite seam in the studied section.

CONCLUSIONS

- The commonest type of stylolite in the study area is the Sedimentary Bedding Stylolite. Tectonic Stylolites are relatively less developed.
- Different types and sets of veins and faults with different age relationship relative to the stylolites were identified. The orthogonal veins with syntaxial fibrous fill are the dominant type, formed as a result of vertical maximum compression and horizontal minimum compression. The syntaxial fibrous growth is believed to be synchronous with the development of the Sedimentary Stylolites.
- The stylolite seam residual deposits consist of quartz, orthoclase, illite and glauconite with calcite and pyrite cements. Bituminous material is common in the seam deposits, indicating originally porous and permeable bedding plain domain at different stages of the stylolitization history.
- The least mobilized elements in the limestone dissolution process are Ti, Al and K, followed by Si, Fe, Cr and U, whereas most of Ca, Mg, Mn, Na and Ni were mobilized.
- Limestone mass, reduced by pressure-solution in the study area was estimated by about 5% using chemical criteria. Thickness shortening was estimated by two independent methods by about 15 cm of limestone needed to produce one cm thick stylolite seam in the studied section.

ACKNOWLEDGMENTS

The authors are indebted to Mr. Varoujan K. Sissakian (GEOSURV Expert) for his help in the fieldwork and to Dr. Buthaina S. Al-Jibouri for the identification of fauna and biofacies of the Kometan Formation in the study area. Thanks are due to Miss. Mariamme Kaka, Miss. Basma A. Ahmed, Mr. Hayder H. Taha and Mr. Ali M. Jassim for their help in microscope photography, typing and figures-editing.

REFERENCES

Al-Barzinjy, S.T., 2008. Origin of chert nodules in Kometan Formation from Dokan area, northeastern Iraq. Iraqi Bull. Geol. Min., Vol.4, No.1, p. 95 – 104.

Al-Haimus, A.F., 1994. GEOSURV Work Procedures, Part 19: Engineering Geology Laboratories. GEOSURV, int. rep. no. 2000.

Al-Janabi, Y., Al-Sa'adi, N., Zainal, Y., Al-Bassam, K. and Al-Delaimy, M., 1992. GEOSURV Work Procedures, Part 21: Chemical Laboratories. GEOSURV, int. rep. no. 2002.

Balaky, S.M., 2006. Digenetic history of the Harur Formation, Early Carboniferous (Tournaisian), Northern Iraqi Kurdistan Region. Iraqi Bull. Geol. Min., Vol.2, No.2, p. 83 – 102.

Bencini, A. and Turi, L., 1974. Mn distribution in the Mesozoic carbonate rocks from Lima Valley, Northern Apennines Jour. Sed. Petr., Vol.44, p. 774 – 782.

Daoud, H.S., Balc, R. and Sur, G.H., 2010. Microfossil assemblages and digenesis of Balambo Formation from Azmer Mountain in Northeast Sulaimaniyah, Kurdistan Region, Iraq. Iraqi Bull. Geol. Min., Vol.6, No.2, p. 1 – 16.

Dunne, W.M. and Hancock, P.L., 1994. Paleostress analysis of small-scale brittle structures. In: P.L. Hancock (Ed.), Continental Deformation. Pergamon Press, Oxford, p. 101 – 120.

Durney, D.W. and Ramsey, J.G., 1973. Incremental strains measured by syntectonic crystal growth. In: K.A. De Jong and R. Scholten (Eds.), Gravity and Tectonics. J. Wiley, New York, p. 67 – 95.

Fouad, S.F.A., 1983. Structural geology of Qara Chuq folds. Unpub. M.Sc. Thesis. University of Baghdad.

Gad, M.A., 1969. Geochemistry of Whitbian sediments of the Yorkshire Coast. Proc. Yorkshire Geol. Soc., Vol.37, p. 105 – 139.

Hancock, P.L. and Atiya, M.S., 1975. The development of en-echelon veins segmented by the pressure solution of formerly continuous veins. Proc. Geol. Assoc., Vol.86, p. 281 – 286.

Jassim, S.Z. and Goff, J.C., 2006 (Eds.) Geology of Iraq. Dolin, Prgue and Moravian Museum, Brno. 341pp.

Korfali, S.I. and Davies, B.D.E., 2004. The relationships of metals in river sediments (Nahr-Ibrahim, Lebanon) and adjacent floodplain soils. Agricultural Engineering International. The CIGR Jour. Sci. Res. Dev., Vol.6, p. 1 – 22.

Kreidler, E.R. and Hummel, F.A., 1970. The crystal chemistry of apatite. Structure field of fluor-and chlorapatite. Am. Miner., Vol.55, p. 107 – 184

Lindsay, W.L., 1979. Chemical Equilibria in Soils. J. Wiley, New York.

Lougheed, M.S. and Mancuso, J.J., 1973. Hematite Framboids in the Negaunee Jorn Formation. Michigan. Evidence for their biogenic origin. Econ. Geol., Vol.68, p. 202 – 209.

Park, W.C. and Schot, E.H., 1968. Stylolites: Their nature and origin. Jour. Sed. Petr., Vol.38, p. 175 – 191.

Ramsey, J.G. and Huber, M.I., 1983. The Techniques of Modern Structural Geology. Vol.1. Strain Analysis. Academic Press, London, 307pp.

Ramsey, J.G. and Huber, M.I., 1987. The Tectonics of Modern Structural Geology. Vol.2. Folds and Fractures. Academic Press, London, 307pp.

Roland, S.M., Duebendorfer, E.M. and Schiefelbein, I.M., 2007. Structural Analysis and Synthesis. Blackwell. Publishing Ltd., USA, 304pp.

Sastri, G.G.K. and Sastry, C.S., 1982. Chemical characteristics and evolution of the laterite profile in Hazaridadar Bauxite Plateau, Madhya Pradesh, India. Econ. Geol., Vol.77, p. 154 – 161.

Schaetzl, R.J. and Anderson, S., 2005. Soils: Genesis and Geomorphology. Cambridge University Press, New York, 791pp.

Sherwani, G.H. and Balaky, S.M., 2006. Black chert, an interesting petrographic component within the upper part of Sargelu Formation (Middle Jurassic), North and Northeastern Iraqi Kurdistan. Iraqi Bull. Geol. Min., Vol.2, No.1, p. 77 – 88.

Suppe, J., 1985. Principles of Structural Geology. Prentice-Hall Inc., New Jersey, 537pp.

Thompson, G.R. and Hower, J., 1975. The mineralogy of glauconite. Clay and Clay Minerals, Vol.23, p. 289 – 300.

Van der Pluijm, B.A. and Marshak, S., 1997. Earth Structure: An Introduction to Structural Geology and Tectonics. WEB/ McGraw-Hill. New York, 495pp.

Veizer, J., Lemienx, J., Jones, B., Gibling, M.R and Savelle, J., 1977. Sodium: Paleosalinity indicator in ancient carbonate rocks. Geology, Vol.5, p. 177 – 179.